Original Article

Secreted Frizzled-related Protein 5 Mediates Wnt5a Expression in Microcystin-leucine-arginine-induced Liver Lipid Metabolism Disorder in Mice*

YANG Mei Yan[1,&], YU Fu Rong[2,&], JI Qian Qian[1], ZHANG Hui Ying[1], ZHANG Jia Xiang[1], and CHEN Dao Jun[1,2,#]

1. Department of Occupational Health and Environmental Health, School of Public Health, Anhui Medical University, Hefei 230032, Anhui, China; 2. School of Medical Technology, Anhui Medical College, Hefei 230601, Anhui, China

Abstract

Objective Microcystin-leucine-arginine (MC-LR) exposure induces lipid metabolism disorders in the liver. Secreted frizzled-related protein 5（SFRP5）is a natural antagonist of winglesstype MMTV integration site family, member 5A (Wnt5a) and an anti-inflammatory adipocytokine. In this study, we aimed to investigate whether MC-LR can induce lipid metabolism disorders in hepatocytes and whether SFRP5, which has anti-inflammatory effects, can alleviate the effects of hepatic lipid metabolism by inhibiting the Wnt5a/Jun N-terminal kinase (JNK) pathway.

Methods We exposed mice to MC-LR in vivo to induce liver lipid metabolism disorders. Subsequently, mouse hepatocytes that overexpressed SFRP5 or did not express SFRP5 were exposed to MC-LR, and the effects of SFRP5 overexpression on inflammation and Wnt5a/JNK activation by MC-LR were observed.

Results MC-LR exposure induced liver lipid metabolism disorders in mice and significantly decreased SFRP5 mRNA and protein levels in a concentration-dependent manner. SFRP5 overexpression in AML12 cells suppressed MC-LR-induced inflammation. Overexpression of SFRP5 also inhibited Wnt5a and phosphorylation of JNK.

Conclusion MC-LR can induce lipid metabolism disorders in mice, and SFRP5 can attenuate lipid metabolism disorders in the mouse liver by inhibiting Wnt5a/JNK signaling.

Key words: Jun N-terminal kinase; Secreted frizzled-related protein 5; Wnt5a; Hepatic lipid metabolism disorder

Biomed Environ Sci, 2024; 37(x): 1-15 *doi: 10.3967/bes2024.081* *ISSN: 0895-3988*

www.besjournal.com (full text) *CN: 11-2816/Q*

INTRODUCTION

In recent years, with global warming, nitrogen, phosphorus, and other organic substances have been discharged into rivers and lakes, resulting in large numbers of algae in the water and endangering the health of aquatic organisms and humans[1]. Microcystin (MC) is a type of cyanobacteria that is one of the most common and dangerous cyanobacterial toxins[2]. There are

*Funds from Natural Science Research Project of colleges and Universities in Anhui Province [2022AH052336] and High Level Talent Research Initiation Fund Of Anhui Medical College [2023RC004].

&These authors contributed equally to this work.

#Correspondence should be addressed to Correspondence should be addressed to CHEN Dao Jun, MD, PhD, E-mail: daodaodao19785@163.com

Biographical notes of the first authors: YANG Mei Yan, female, born in 1997, Master, majoring in biomarkers of environmental health; YU Fu Rong, female, born in 1978, Master, majoring in biomarkers of environmental factors and tumors.

more than 270 MC homologs[3], of which MC-leucine-arginine (MC-LR) is the most toxic and abundant. MC-LR contamination levels in the environment range from 0.1 μg/L to a few mg/L[4]. South Africa is currently the most heavily polluted by MCs in surface water, with 124,460 μg/L detected in its reservoir[5]. The MC-LR in water from Lake Tai in 2007 showed that the maximum concentration was 0.522 μg/L[6]. The highest concentration of MCs in groundwater in Lake Chaohu is 1.07 μg/L[6]. In the high-incidence area of liver cancer, the concentration of MC-LR in pond and ditch water was found to be as high as 1.158 μg/L[7], exceeding the national drinking water limit standard (1 μg/L) specified by the World Health Organization in 1998[2]. MC-LR is considered a tumor promoter in mammals because of its potent inhibitory effects on protein phosphatase 1 and 2A[2]. MC-LR is a metabolism-disrupting chemical that can perturb lipid metabolites and contribute to the development of metabolic syndromes[3]. MC-LR accumulates in the liver mainly through blood circulation. Metabolic disturbances, including fatty acid beta-oxidation and hepatic lipoprotein output, are significantly inhibited in mice after short-term, low-dose MC-LR exposure, resulting in nonalcoholic fatty liver disease[4,8].

Lipid metabolism is closely related to the physiological and pathological status[9]. The liver is the primary organ involved in lipid metabolism in the human body[10]. Fatty acid synthesis, lipid oxidation, and lipolysis are key processes in lipid metabolism[11]. Several studies have shown that long-term intake of low concentrations of MC-LR can lead to liver lipid metabolism disorders, including nonalcoholic fatty liver disease and liver fibrosis[9,12]. The pathogenesis of hepatic steatosis is complex and diverse, involving the environment, genetics, hormone secretion, oxidative stress, immune response, and the intestinal ecological environment[13]. However, these mechanisms need to be elucidated. Therefore, this study is essential for understanding the molecular mechanisms of lipid metabolism in the liver and identifying future therapeutic targets.

Secreted frizzled-related protein 5 (SFRP5), a member of the SFRP family, is an anti-inflammatory adipocytokine[14]. SFRP5 is structurally similar to the frizzled receptor in the Wnt signaling pathway[14] and can inhibit the activity of the Wnt signaling pathway by competitively binding to the frizzled receptor, thereby negatively regulating the Wnt pathway[15]. As an antagonist of the Wnt pathway, SFRP5 acts mainly through the noncanonical Wnt pathway[16].

Wnt5a, a proinflammatory adipokine, is a noncanonical component of the Wnt signaling pathway[17]. Experimental results using animal models have shown that its expression increases in proportion to obesity[17]. The classical molecular mechanism of SFRP5 is to bind to Wnt5a and inhibit the binding of Wnt5a to its receptor, thus blocking downstream Jun N-terminal kinase (JNK) phosphorylation and triggering proinflammatory and proliferative processes[16,18,19].

Some studies have shown that SFRP5 knockout mice develop obesity and fatty inflammation, and that overexpression of SFRP5 by adenovirus can alleviate obesity, fatty inflammation, and hepatic steatosis[20]. In vitro, administration of SFRP5 ameliorates hepatic lipid accumulation, inflammation, and nonalcoholic steatohepatitis[21,22]. However, it is unclear whether SFRP5 plays an important role in MC-LR-induced liver fat metabolism disorders, or the mechanism by which it regulates downstream molecules.

In the present study, we injected MC-LR into

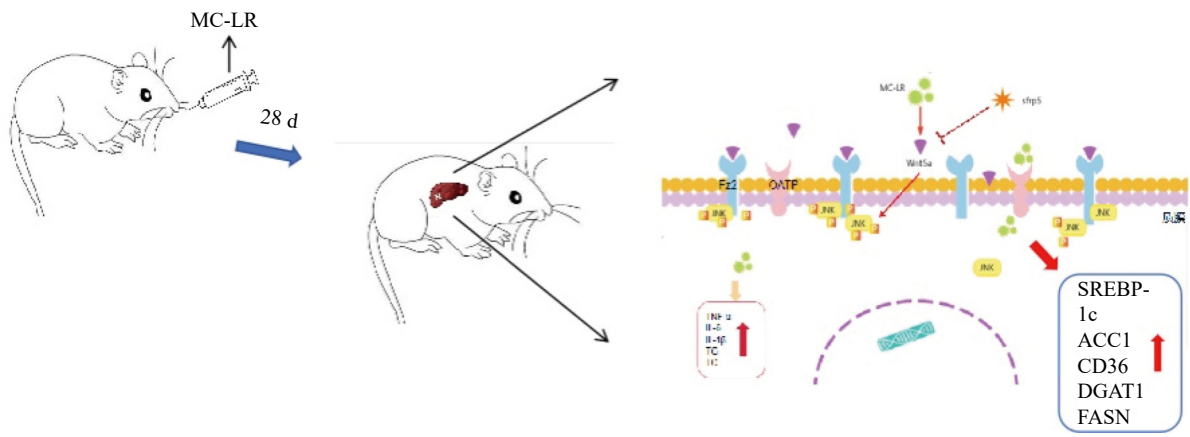

Supplementary Figure S1. Supplemental Figure S1. Schematic diagram of the experimental method.

mice daily to induce a liver injury model, and liver inflammation in mice was aggravated to produce liver lipid metabolism disorders. However, by overexpressing SFRP5, the effects of the Wnt5a pathway and phosphorylated JNK (p-JNK) were observed, and their roles in liver lipid metabolism disorders were investigated.

METHODS

Experimental Animal

Forty specific pathogen-free male BALB/C mice of 6–8 weeks old and weighing 18–20 g, were purchased from the Anhui Experimental Animal Center. The mice were housed in the animal room of Anhui Medical University for 30 days. The temperature was maintained at 20–25 °C, the humidity was controlled in the range of (50% ± 5%, the circadian rhythm of light/dark was manually controlled for 12 hours, and the mice were allowed to eat and drink freely. All animal experiments were performed in accordance with the guidelines of the Institutional Animal Care and Use Committee (IACUCUNK1). After a week of adaptive feeding, the mice were randomly divided into a control group, 50 μg/kg per day MC-LR group, a 100 μg/kg per day MC-LR group, and a 200 μg/kg per day MC-LR group, with 10 mice in each group. The mice were fed at 12 o'clock every day for 28 days, and feeding was stopped 24 h before euthanizing the mice (Supplemental Figure S1, www.besjjournal.com).

Cell Culture

Cells were cultured in 10% fetal bovine serum (GIBCO, USA) and 1% penicillin-streptomycin (Beyotime, China) in RPMI 1640 medium (DMEM) (GIBCO.USA) with a 1% insulin-transferrin-selenium (Beyotime, China) additive. The culture dish was placed in an incubator at 37 ° C and 5% CO2, and the medium was changed every 24 hours and the cell growth was observed. After 72 h, the cells were digested and passaged, and the protein, RNA, and supernatants of the third-generation cells were collected and extracted for subsequent experiments.

Biochemical Index Detection

The serum of the mice was centrifuged and measured according to the manufacturer's instructions for aspartate aminotransferase (AST), alanine aminotransferase (ALT), high-density lipoprotein cholesterol (HDL-C), low-density lipoprotein cholesterol (LDL-C), total cholesterol (TC), and total triglyceride (TG) detection kits (Jiancheng Biology, China). Interleukin-6 (IL-6), interleukin-1β (IL-1β), tumor necrosis factor-α (TNF-α), interleukin-4 (IL-4), and interleukin-10 (IL-10) (Calvin, China) levels were analyzed by enzyme-linked immunosorbent assay (ELISA).

Liver Pathology

Mouse livers were embedded in paraffin and sectioned after exposure to MC-LR. Paraffin sections of 5 μm were stained with hematoxylin and eosin (Solarbio, China) to observe mouse liver inflammation and balloon-like lesions of hepatocytes.

Cell Transfection

Cells were seeded at 1×10^6 cells/well in 6-well plates prior to transfection and transfected when cultured to 70%–90% confluency. According to the manufacturer's instructions, Lipofectamine 3000 (Thermo Fisher Scientific, USA) plus 5 μg of a pEGFP vector (Sangon Biotech Co., Ltd, China) containing SFRP5 (OV-SFRP5) or the empty vector (OV-NC) were used for transfection, incubated for 48 hours at 37 ° C in a 5% CO_2 incubator.

Cell counting kit-8 (CCK-8)

After treatment, cell viability was determined using the CCK-8 assay (Beyotime, China). The cells were seeded in a 96-well plate at a density of 2×10^3 cells/well and incubated overnight at 37 °C. Subsequently, 10 μL of CCK-8 solution was added, and the cells were cultured for 2 h at 37 °C. The absorbance was measured at 450 nm using a microplate reader (Bio-Rad, Hercules, CA, USA).

Western Blot

Proteins in the mouse liver and cells were extracted with radioimmunoprecipitation assay lysis buffer (Beyotime, China), and total protein concentration was quantified using a bicinchoninic acid protein assay kit (Beyotime, China). A total of 35 μg of protein was transferred to sodium dodecyl sulfate-polyacrylamide gel electrophoresis, and then further transferred to a polyvinylidene fluoride membrane (Millipore, USA). They were then incubated with anti-glyceraldehyde-3-phosphate dehydrogenase, anti-SFRP5, anti-Wnt5a, anti-JNK, anti-P-JNK, anti-β-catenin, and anti-Wnt3a (SANTA, USA) for 12 hours at 4 °C, followed by incubation with horseradish peroxidase-conjugated anti-mouse antibody for 1 h at 37 °C. The protein bands were visualized by enhanced chemiluminescence

detection and analyzed using Image-Pro Plus software.

Real-time Quantitative Polymerase Chain Reaction

Total RNA was extracted from the cells and mouse liver tissues using TRIzol reagent (Invitrogen, USA). Total RNA was reverse transcribed into complementary DNA using PrimeScript™ RT reagent Kit (Roche, China). Quantitative polymerase chain reaction was performed using 1 ml of complementary DNA per well, TaqMan Master Mix (Applied Biosystems), and 20 mmol/L each of the sense and antisense primers. The results were evaluated using the method, and the calculated number of copies was normalized to the number of glyceraldehyde-3-phosphate dehydrogenase mRNA copies in the same sample. The primers used in this study are listed in Table 1.

Statistical Analysis

In this study, quantitative variables are expressed as the mean ± standard deviation, GraphPad Prism 8.4 (GraphPad, California, USA) software was used for statistical analysis. One-way analysis of variance was used to evaluate differences between groups. A value of $P < 0.05$ was considered statistically significant.

RESULTS

Effects of MC-LR on Body Weight and Liver Coefficient in Mice

There was no significant difference in the body weight of the mice as a whole; however, the body weight of the blank control group increased slowly. Before the 18th day of exposure, the body weight of mice in all groups increased, and the body weight of mice in the 50, 100, and 200 μg/kg per day MC-LR groups was significantly higher than that of the control group. After the 18th day, the body weight of the mice in the 50, 100, and 200 μg/kg per day MC-LR groups began to decrease, and the body weight of the mice in the experimental groups was lower than that of the control group, especially in the 50 μg/kg per day MC-LR group (Figure 1). However, there were no significant changes in the liver coefficients of mice (Figure 2). These data indicate that there was no significant change in the overall outward performance trend of MC-LR in the short term compared with that in the blank control group.

Serum Biochemical Indexes of Mice

To further study the effect of MC-LR on liver fat metabolism in mice, we collected blood from mice, centrifuged the serum, and detected the levels of high-density lipid-cholesterol (HDL-C), low-density lipid-cholesterol (LDL-C), TC, TG, alanine transaminase (ALT), and aspartate transaminase (AST) in the serum of mice (Figure 3). The serum levels of HDL-C, LDL-C, TC, and TG in the high-dose 200 μg/kg per day MC-LR group were significantly higher than those in the other groups and the control group, with significant differences compared to the control group. ALT was significantly increased in the MC-LR trial group and was statistically significant. The AST content in the serum of the 100 and 200 μg/kg per day MC-LR groups was

Table 1. RNA primer

Primer	Forward Primer (5′–3′)	Reverse Primer (5′–3′)
SREBP-1c	TGGAGACATCGCAAACAAG	GGTAGACAACAGCCGCATC
ACC1	AAGGGACAGTAGAAATCAAA	CAGCCTCCAGTAGAAGAAG
FASN	GCCTCCGTGGACCTTATC	ACAGACACCTTCCCGTCA
SCD1	GGGAATAGTCAAGAGGCT	ACGAGGACGACAATACAA
CD36	GGCAGGAGTGCTGGATTA	GAGGCGGGCATAGTATCA
DGAT1	GTGGGTTCCGTGTTTGC	CTCGGTAGGTCAGGTTGTCT
SFRP5	CACTGCCACAAGTTCCCCC	TCTGTTCCATGAGGCCATCAG
Wnt5a	CAACTGGCAGGACTTTCTCAA	CCTTCTCCAATGTACTGCATGTG
GAPDH	TCGGAGTCAACGGATTTGGT	TGAAGGGGTCATTGATGGCA

Note. *SREBP-1c*, sterol regulatory element-binding transcription factor-1c; *ACC1*, acetyl-CoA carboxylase 1; *FASN*, fatty acid synthase; *SCD1*, stearoyl-CoA desaturase-1; *CD36*, cluster of differentiation 36; *DGAT1*, diacylglycerol o-acyltransferase 1; *SFRP5*, secreted frizzled-related protein 5; *GAPDH*, glyceraldehyde-3-phosphate dehydrogenase.

significantly higher than that of the control group.

Pathological Observation of Mouse Liver

The effects of different MC-LR doses on the livers of mice are shown in Figure 4 (A and B). No apparent liver injury was observed in the group that did not receive MC-LR treatment. There was slight infiltration of inflammatory cells and disarrangement of hepatic lobules in the 50 μg/kg per day MC-LR treated group. However, 100 and 200 μg/kg per day MC-LR showed obvious inflammatory soaking and a disordered arrangement of the hepatic lobules. It is worth noting that through hematoxylin and eosin staining, different degrees of steatosis of hepatocytes were found in the 50, 100, and 200 μg/kg per day MC-LR treatment groups, and the hepatocytes were filled with lipid vacuoles of different sizes, which was more evident in the 200 μg/kg per day high dose group. No significant difference was observed in the control group.

Effect of MC-LR on Hepatic Inflammation

As shown in Figure 5 and 6, after the mice were exposed to MC-LR for 28 days, the proinflammatory factors IL-6, IL-1β, and TNF-α were positively correlated with the increase in exposure dose, and there was statistical significance. Similarly, levels of the anti-inflammatory factor IL-4 decreased gradually with increasing exposure doses. IL-10, an anti-inflammatory factor, showed a slightly downward trend.

Effect of MC-LR on Hepatic Lipid Metabolism

To determine whether MC-LR exacerbates hepatic lipid metabolism disorders in mice, the relative mRNA expression levels of lipid synthesis-related genes and fatty acid β-oxidation-related genes were examined by polymerase chain reaction (Figure 7). Compared with the control group, the expression levels of lipid synthesis-related genes, such as sterol regulatory element-binding transcription factor-1c (SREBP-1c), acetyl coenzyme a carboxylase 1 (ACC1), fatty acid synthase (FASN), cluster of differentiation 36 (CD36), peroxisome proliferator-activated receptor gamma, stearoyl-CoA desaturase-1, and diacylglycerol O-acyltransferase 1, in the 100 and 200 μg/kgper day MC-LR treatment groups were significantly upregulated. However, a downward trend was observed in the 50 μg/kg per day MC-LR treatment group.

Expression Levels of SFRP5 and Wnt5a in MC-LR exposed Mice and Mouse Hepatocytes (AML12)

To determine whether SFRP5 is involved in lipid metabolism disorders and hepatocyte damage induced by MC-LR exposure in mice, we measured the mRNA (Figure 8A) and protein (Figure 8B) expression levels of SFRP5 after exposure to different concentrations of MC-LR. This expression levels in cells are shown in Figure 9. Compared to the control group, the mRNA and protein levels of SFRP5 were significantly decreased, and the mRNA and protein levels of Wnt5a tended to decrease. As expected, our results suggested that SFRP5 may play a role in MC-LR-induced hepatic lipid metabolism disorders. In addition, considering the decrease in cell viability caused by MC-LR, an exposure time of 24 hours and an exposure dose of 1 μmol/L MC-LR were selected for subsequent experiments (Figure 10).

Overexpression of SFRP5 Inhibits MC-LR-induced Inflammation in AML12 Cells

Subsequently, cells transfected with OV-SFRP5 and OV-NC cells served as controls. The successful overexpression of SFRP5 in AML12 cells was verified, as shown in Figure 11. The expression of

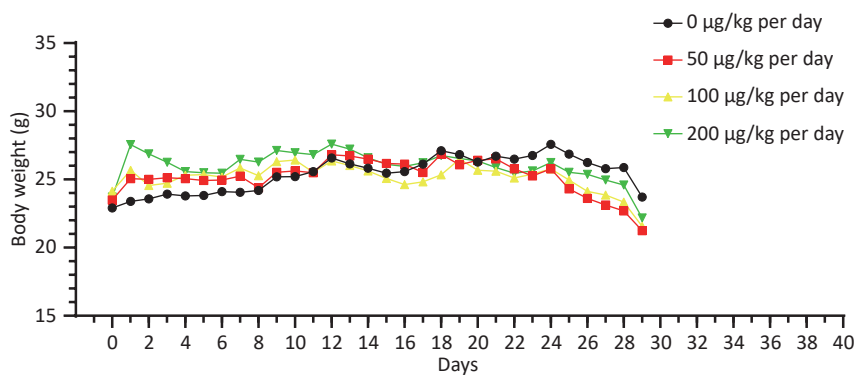

Figure 1. The body weight change trend after being exposed to microcystin-leucine-arginine for 28 days (*n* = 7).

inflammatory factors in cells overexpressing SFRP5 was then measured. As depicted in Figure 12, MC-LR significantly increased the levels of IL-6, IL-1β, and TNF-α. However, SFRP5 overexpression significantly reduced the concentration of these cytokines.

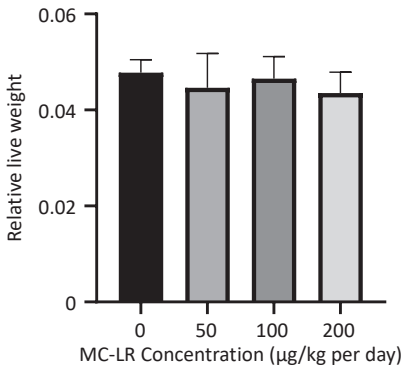

Figure 2. Effects of microcystin-leucine-arginine on the livers of mice. Absolute liver weights in different groups (n = 7).

Overexpression of SFRP5 Inhibits Wnt5a-induced Phosphorylation of JNK

To investigate whether SFRPR exposure to MC-LR affected the Wnt5a/JNK pathway, we measured the protein expression of Wnt5a, JNK, P-JNK, and Wnt3a in hepatocytes transfected with OV-SFRP5. The results indicated that the OV-SFRP5 group significantly inhibited the expression of Wnt5a and P-JNK compared with the MC-LR group (Figure 13). These data suggest that SFRP5 inhibits the Wnt5a/JNK pathway, thereby preventing MC-LR from inducing lipid metabolism disorders and liver inflammation.

DISCUSSION

With problems, such as human activities and global warming, rivers and lakes are becoming

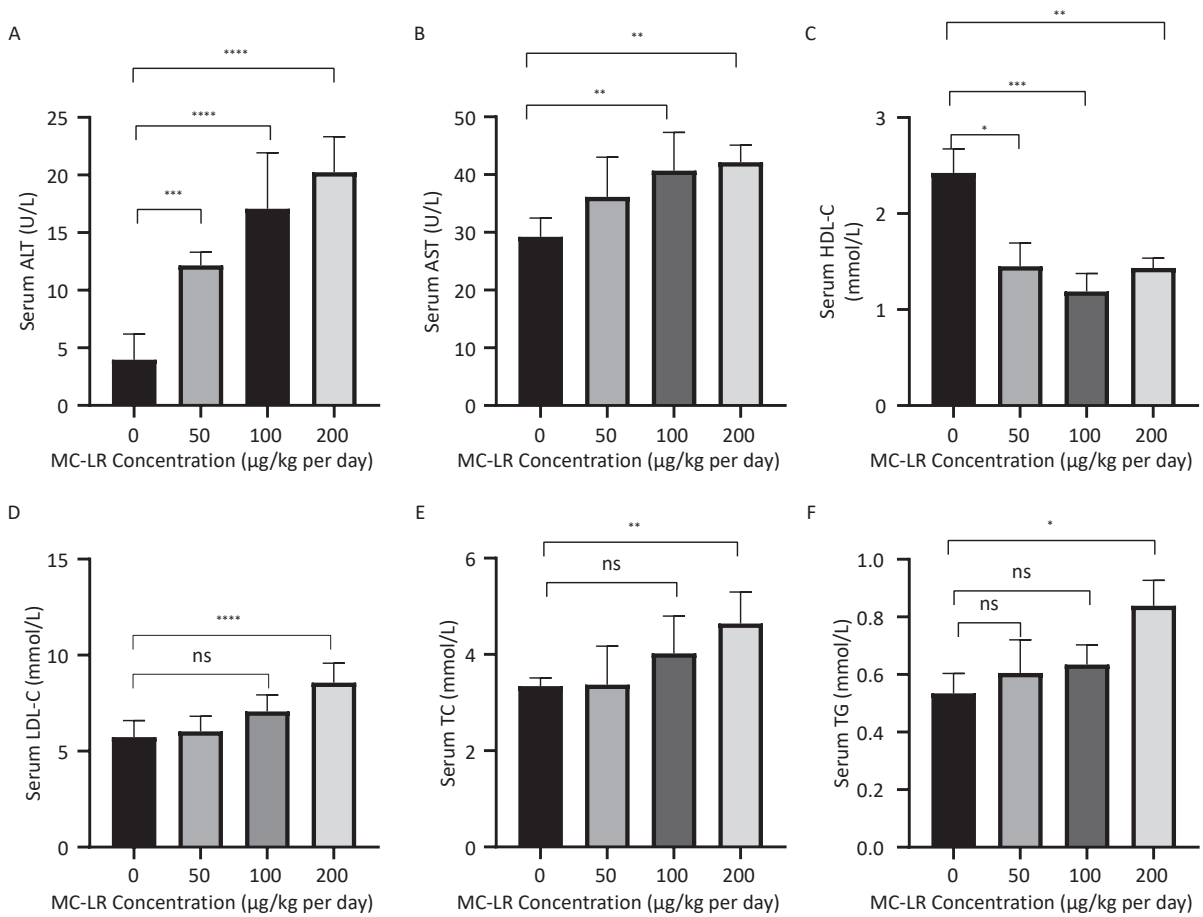

Figure 3. The effects of microcystin-leucine-arginine on serum ALT (A), AST(B), HDL-C(C), LDL-C(D), TC(E), and TG(F) levels in mice (n = 7). HDL-C, high-density lipoprotein cholesterol; LDL-C, low-density lipid cholesterol; TC, total cholesterol; TG, triglyceride; ALT, alanine transaminase; AST, aspartate transaminase; $^{*}P < 0.05$; $^{**}P < 0.01$; $^{***}P < 0.001$; $^{****}P < 0.0001$; ns, no significance.

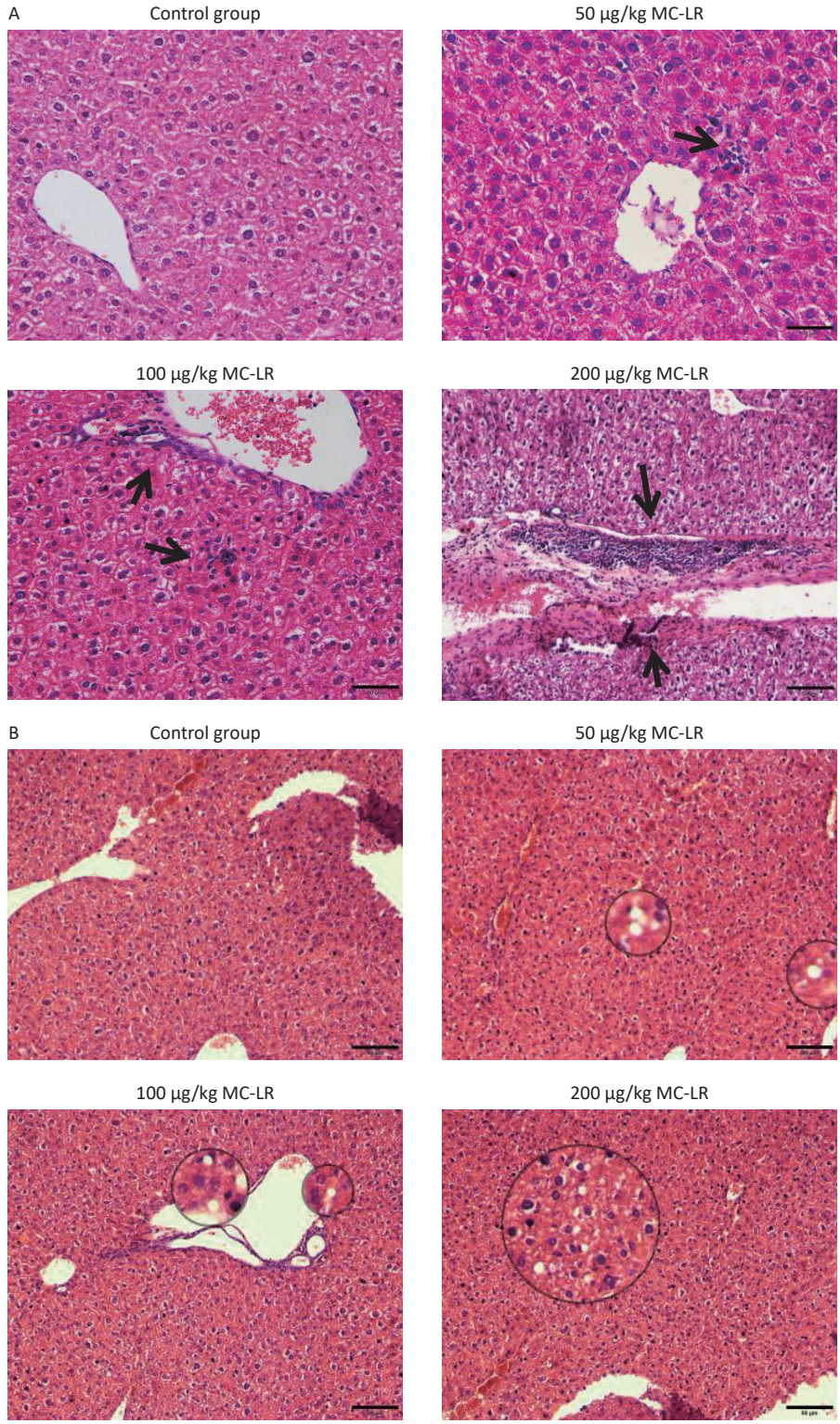

Figure 4. Histological observations of the livers of mice treated with different doses of microcystin-leucine-arginine (200× magnification, scale bar = 150 μm). (A) Hematoxylin and eosin staining observed Inflammatory cell infiltration of mice liver microstructure in various groups. The black arrow indicates infiltrating inflammatory cells. (B) Hematoxylin and eosin staining observed the fat vacuoles of mice liver microstructure in various groups.

eutrophic, leading to increased cyanobacteria blooms, and cyanobacterial toxins that endanger aquatic organisms and can cause serious harm to human health. MC-LR has been identified as a class 2B carcinogen[23]. Nevertheless, most studies on MC-LR to date have focused on liver inflammation or long-term low-dose continuous[24] or intermittent exposure through drinking water[25], leading to liver lipid metabolism disorders. Few studies have investigated the effects of intragastric administration of MC-LR on liver lipid metabolism in mice. Therefore, in our study, mice were given 50, 100, and 200 μg /kg per day MC-LR for 28 days. Studies have shown that short-term high-dose exposure to MC-LR can lead to liver inflammation and lipid metabolism disorders.

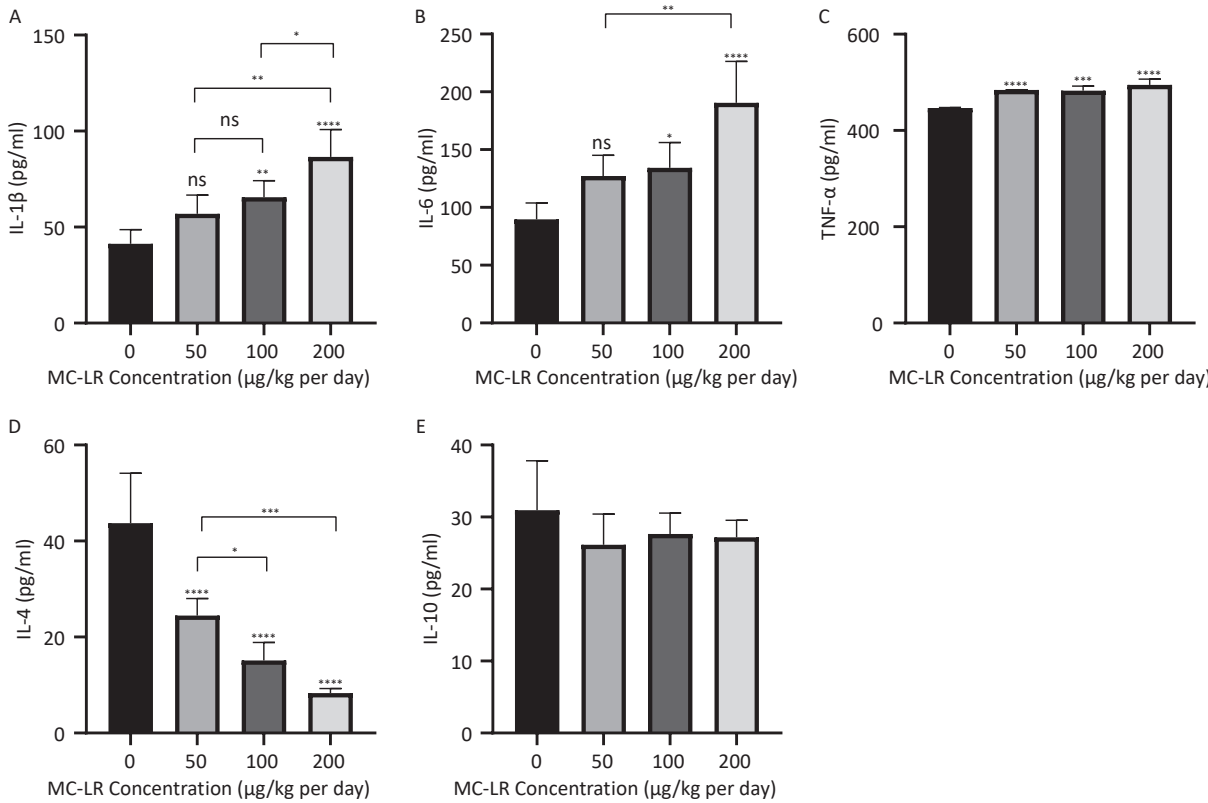

Figure 5. Different groups' expression levels of the inflammatory factors IL-1β (A), IL-6 (B), and TNF-α (C), and anti-inflammatory factors IL-4 (D) and IL-10 (E) by ELISA (n = 7). IL-6, interleukin-6; IL-1β, interleukin-1β; TNF-α, tumor necrosis factor-α; IL-4, interleukin-4; IL-10, interleukin-10; ELISA, enzyme-linked immunosorbent assay; $^{*}P < 0.05$; $^{**}P < 0.01$; $^{***}P < 0.001$; $^{****}P < 0.001$; ns, no significance.

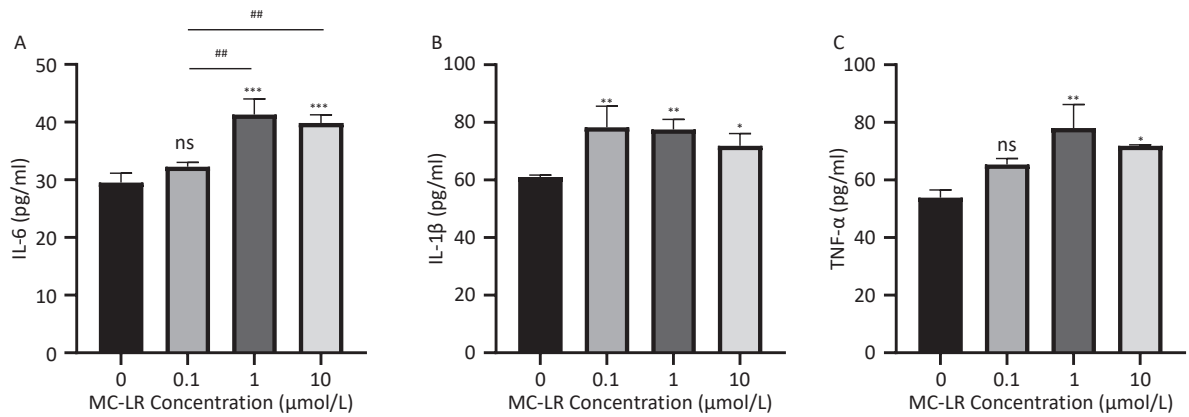

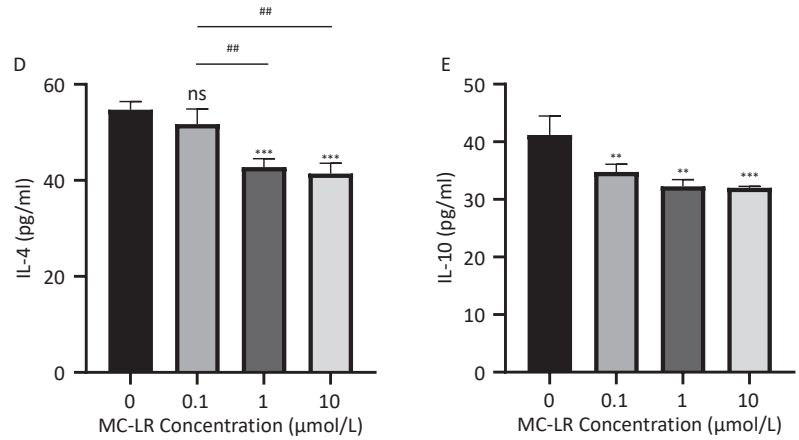

Figure 6. Different groups' expression levels of the inflammatory factors IL-6 (A), IL-1β (B), and TNF-α (C), and anti-inflammatory factor IL-4 (D) and IL-10 (E) by ELISA (*n* = 3). IL-6, interleukin-6; IL-1β,interleukin-1β; TNF-α, tumor necrosis factor-α ; IL-4, interleukin-4; IL-10, interleukin-10; ELISA, enzyme-linked immunosorbent assay; $^{*}P < 0.05$; $^{**}P < 0.01$; $^{****}P < 0.001$; ns, no significance

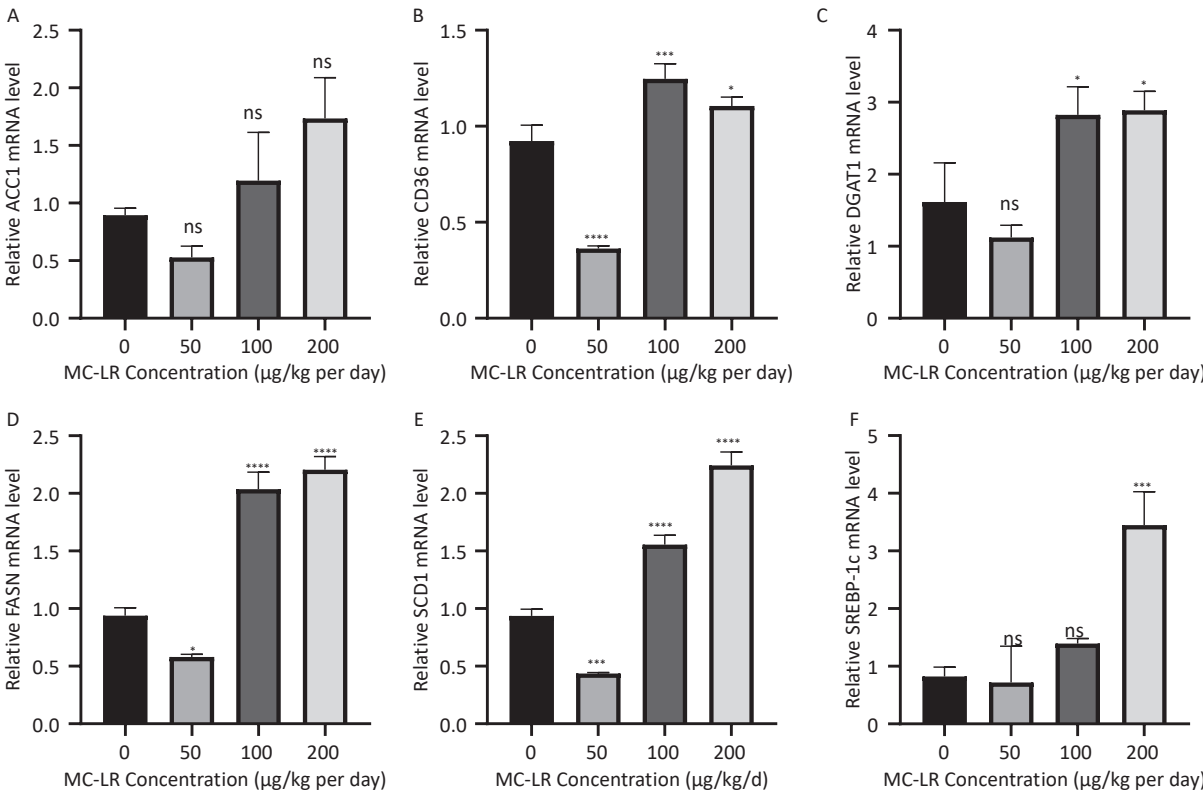

Figure 7. The effects of microcystin-leucine-arginine on the lipid β-oxidation related genes mRNA expression levels in the liver of mice. (A) ACC1 mRNA expression levels in various groups; (B) CD36 mRNA expression levels in various groups; (C) DGAT1 mRNA expression levels in various groups; (D) FASN mRNA expression levels in various groups; (E) SCD1 mRNA expression levels in various groups; (F) SREBP-1c mRNA expression levels in various groups. (*n* = 7). SREBP-1c, sterol regulatory element-binding transcription factor-1c; ACC1, acetyl coenzyme A carboxylase 1; FASN, fatty acid synthase; SCD1, stearoyl-CoA desaturase-1; CD36, cluster of differentiation 36; DGAT1, diacylglycerol o-acyltransferase 1; $^{*}P < 0.05$; $^{**}P < 0.01$; $^{***}P < 0.001$; $^{****}P < 0.001$; ns, no significance

Effect of MC-LR on the General Condition of Mice

In this study, different doses of MC-LR were administered to the mice by gavage. There was no significant change in the body weight of the mice after 28 days; however, there was a slight change in the body weight trend of each group before and after 18 days, which may indicate the severe impact of MC-LR on the mice. Similarly, there was no significant change in the liver coefficient of mice in the treatment groups compared with that in the control group. These data suggest that MC-LR had no significant effect on mouse body weight or liver.

Effect of MC-LR on Hepatic Inflammation in Mice

Because AST and ALT are essential indicators of liver function, their levels increase when liver cells are damaged, and the degree of increase is positively correlated with the degree of liver cell damage[26]. Compared with the control group, the levels of AST and ALT in the serum of mice increased, indicating liver damage. MC-LR can cause histopathological injury to the mouse liver, such as disorders of hepatic lobules, prominent infiltration of inflammatory cells, and fatty degeneration of hepatocytes[27,28]. These results indicate that MC-LR induces liver injury in mice.

Effect of MC-LR on Lipid Metabolism in Mouse Liver

From the perspective of biochemical tests, the increase in serum TG, TC, LDL-c, and liver TG and TC, and the decrease in serum HDL-c in mice were caused by MC-LR, consistent with our previous hypothesis. Histopathologically, the hepatocytes of the mice showed fat vacuoles. These results indicate that MC-LR significantly enhanced lipid deposition in mouse hepatocytes. Lipid metabolism involves lipid synthesis and fatty acid β-oxidation. The de novo synthesis of fatty acids (DNL) is an essential biosynthetic pathway in the liver that contributes to

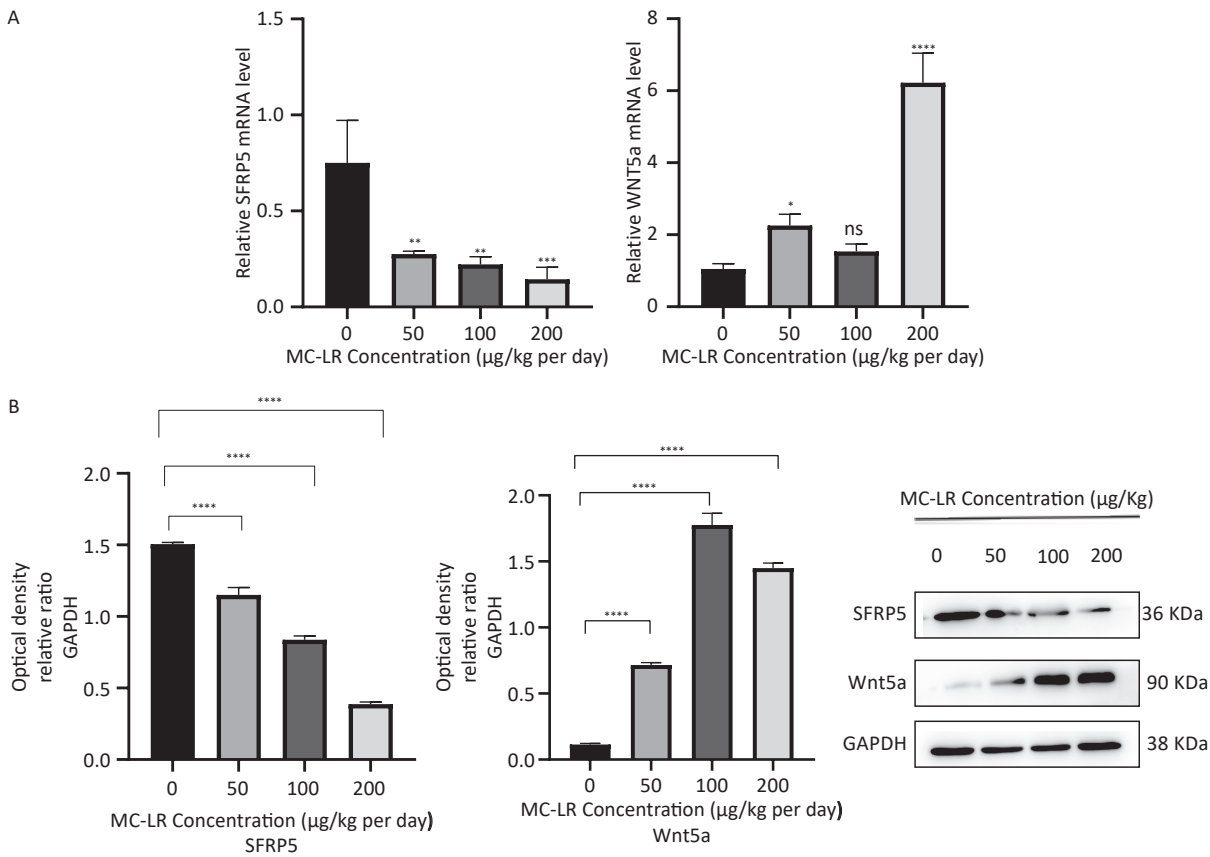

Figure 8. (A) Expression of SFRP5 and Wnt5a mRNA in mice with MC-LR-induced liver injury. (B) The effects of MC-LR on the protein expression levels of Wnt5a and SFRP5 in the liver of mice across various groups. SFRP5, secreted frizzled-related protein 5; GAPDH, glyceraldehyde-3-phosphate dehydrogenase; MC-LR, microcystin-leucine-arginine; GAPDH, glyceraldehyde-3-phosphate dehydrogenase; $^{*}P < 0.05$; $^{**}P < 0.01$; $^{***}P < 0.001$; $^{****}P < 0.0001$; ns, no significance.

the storage and secretion of lipids[29]. This process is regulated by multiple factors within the hepatocytes. A significant pathway regulating the initiation of fatty acid metabolism in the liver involves the stimulation of SREBP-1c expression, a key factor in hepatic lipid synthesis[27]. SREBP1-c, a steroid regulatory element-binding protein, is a crucial regulator of endogenous fatty acid synthesis in hepatocytes. Mature SREBP-1c is transferred to the nucleus to promote fatty acid biosynthesis by upregulating the expression of lipogenesis-related genes, including *SCD1* and *ACC1*[26]. SCD1 is an enzyme located in the endoplasmic reticulum that catalyzes the formation of monounsaturated fatty acids from 12- to 18-carbon saturated fatty acids[27,28]. ACC1 is an essential rate-limiting enzyme involved in fatty acid metabolism[30]. ACCs catalyze the carboxylation of acetyl-CoA to produce malonyl-CoA, which is utilized by FASN to produce long-chain saturated fatty acids[30,31]. In the cytoplasm, ACC1 is primarily responsible for converting cytoplasmic acetyl-CoA to malonyl-CoA for fatty acid synthesis[31]. FASN is a multienzyme protein that is a crucial regulator of lipid metabolism, especially fatty acid synthesis[31,32]. FASN UNK1 converts glucose to fatty acids[33]. The outer ring of CD36 contains a large hydrophobic cavity that provides a docking site for fatty acids and other hydrophobic ligands, facilitating the attraction of hydrophobic ligands to the cell surface and thus promoting the transportation of fatty acids into the cell[34]. CD36 is a scavenger receptor involved in lipid metabolism[35].

The Wnt Pathway is Generally divided into Canonical and Noncanonical Signaling.

Nonclassical Wnt signaling is defined by a β-catenin-independent signaling mechanism[36]. Glycogen synthase kinase-3β (GSK-3β) plays a role in many cellular processes, including cell proliferation, DNA repair, cell cycle, signaling, and metabolic pathways[37]. The role of GSK-3β in the Wnt/β-catenin pathway is to regulate the function of β-catenin by mediating its phosphorylation[38]. GSK-3β and P-GSK-3β play a key role in the classical Wnt signaling pathway[15]. SFRP5 antagonizes the transduction of the Wnt5a noncanonical signaling pathway, thus contributing to the production of anti-inflammatory cytokines[39]. This negative feedback

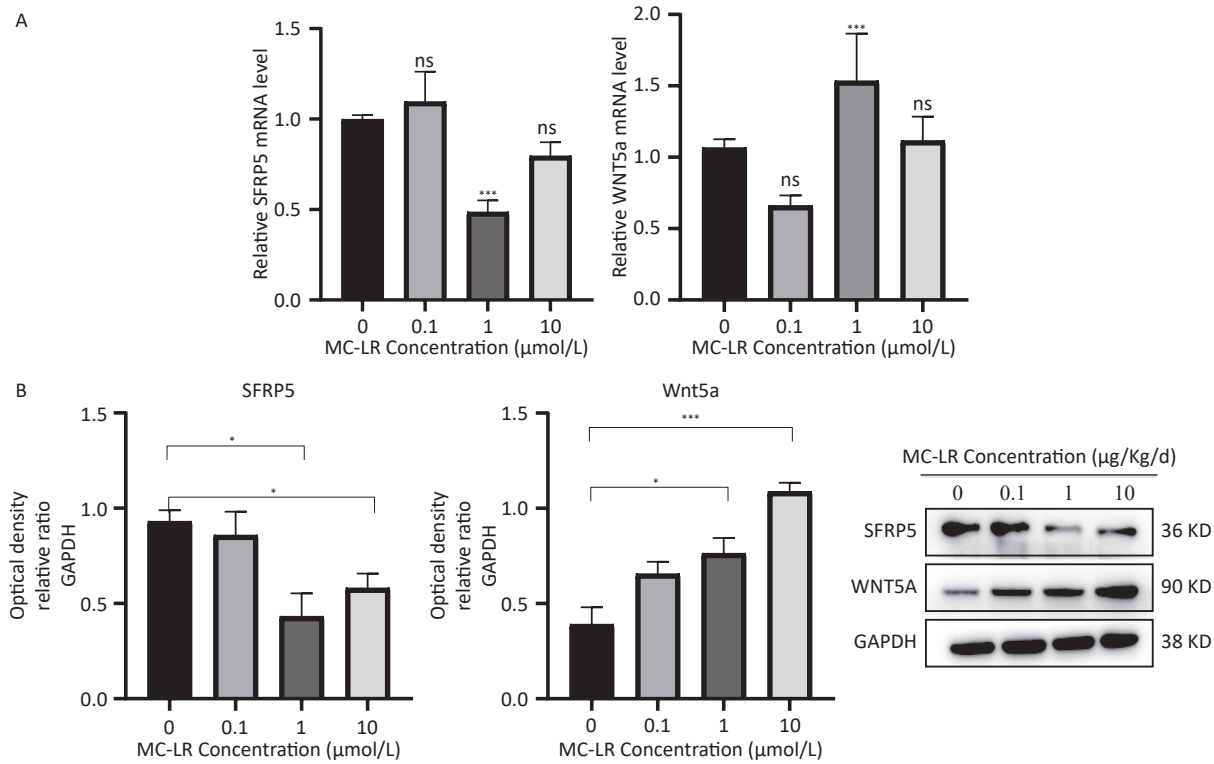

Figure 9. Effects of MC-LR on mRNA and protein expression levels in AML12 cells. Expression levels of Wnt5a and SFRP5 proteins across various groups. SFRP5, secreted frizzle-related protein 5; GAPDH, glyceraldehyde-3-phosphate dehydrogenase; MC-LR, microcystin-leucine-arginine; $^{*}P < 0.05$; $^{***}P < 0.001$; ns, no significance.

mechanism further increases Wnt signaling as SFRP5 expression is reduced[16]. Wnt5a expression was significantly attenuated by SFRP5 overexpression, suggesting that SFRP5 attenuates MC-LR-induced hepatocyte injury by inhibiting Wnt5a expression. Wnt5a expression is proportional to obesity and activates JNK in macrophages and adipocytes[40]. Furthermore, we found that overexpression of SFRP5 in AML12 cells downregulated the phosphorylated form of JNK, a downstream target of noncanonical Wnt signaling. These results indicate that overexpression of SFRP5 in hepatocytes reverses activated Wnt/JNK signaling and inhibits the expression of proinflammatory mediators, as well as the development of lipid metabolism disorders, suggesting that the SFRP5/Wnt5a/JNK regulatory axis is a potential target for hepatocytes.

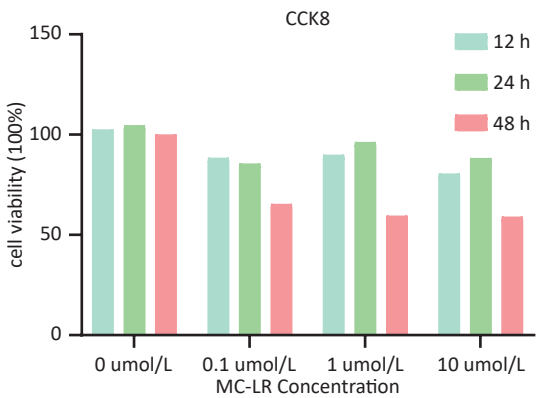

Figure 10. Viability of AML12 cells exposed to different concentrations of MC-LR (n = 5). CCK8, Cell counting kit-8; MC-LR, microcystin-leucine-arginine.

CONCLUSION

In conclusion, our results indicate that continuous intragastric administration of MC-LR for 28 days in mice induces liver inflammation and hepatic lipid metabolism disorders. The primary mechanism is that SFRP5 significantly affects the regulation of the inflammatory response and the downregulation of JNK signaling in hepatocytes. Although the exact mechanism remains to be elucidated, our results suggest a novel role for SFRP5 as a negative regulator of liver injury in mice, providing a scientific basis for further studies on hepatotoxicity, which can help prevent severe liver disease caused by MC-LR.

ETHICS STATEMENT

The animal study protocol was reviewed and approved by the Experimental Animal Ethics Committee of Anhui Medical College (No. 2022-LLBG-021)

ACKNOWLEDGMENTS

We thank our colleagues at the Department of Occupational Health and Environmental Health, School of Public Health, Anhui Medical University for their support in the imaging process. Additionally, we thanks all our colleagues who participated in this

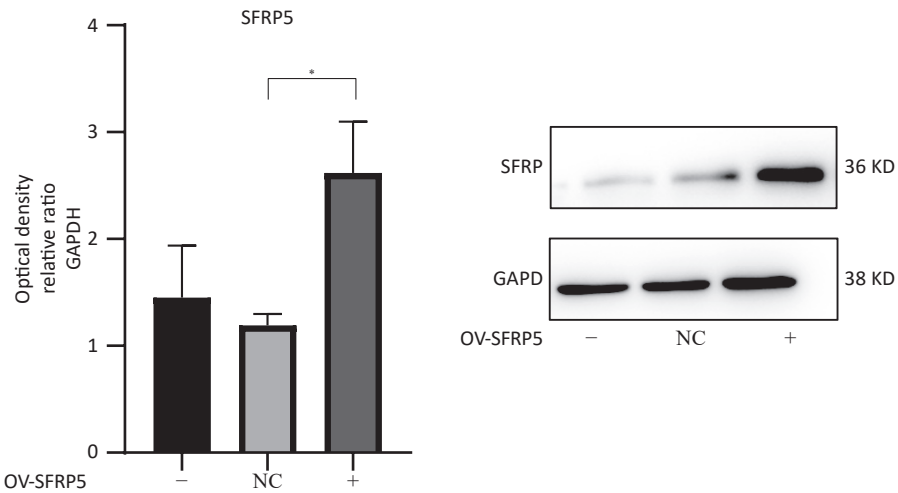

Figure 11. Protein expression of SFRP5 in AML12 cells transfected with NC or OV-SFRP5 vectors. SFRP5, secreted frizzled-related protein 5; GAPDH, glyceraldehyde-3-phosphate dehydrogenase; $^{*}P < 0.05$; OV, overexpression; NC, negative control.

study.

AUTHOR CONTRIBUTIONS

YANG Mei Yan and YU Fu Rong prepared the manuscript. YANG Mei Yan, JI Qian Qian, and ZHANG Hui Ying performed the experiments and analyzed the data. YANG Mei Yan and JI Qian Qian performed the related experiments on animals. CHEN Dao Jun and ZHANG Jia Xiang reviewed and revised the manuscript. CHEN Dao Jun and ZHANG Jia Xiang guided the project. All the authors contributed to the manuscript and approved the submitted version.

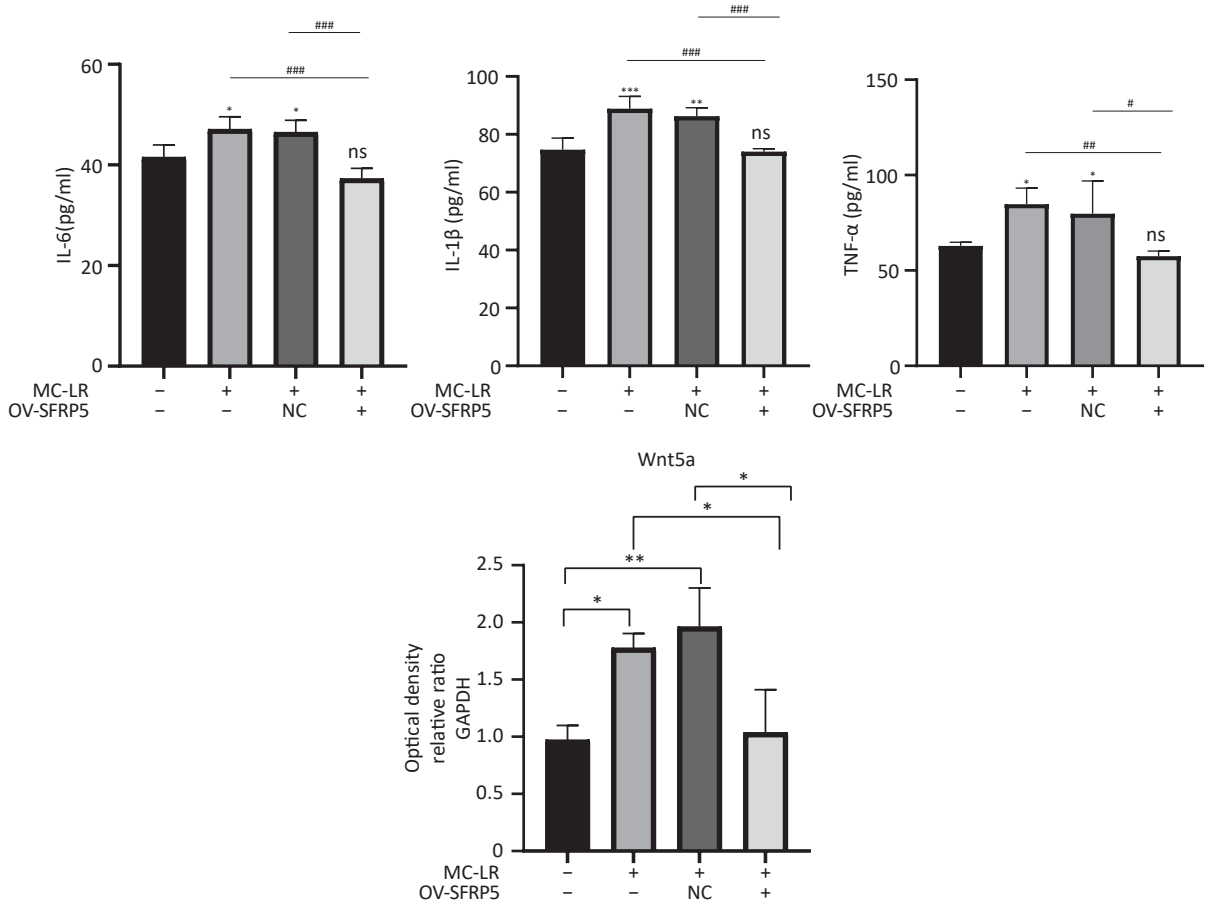

Figure 12. Overexpression of SFRP5 inhibits MC-LR-triggered inflammation in AML12 cells. Concentration of inflammatory factors IL-6, IL-1β, and TNF-α in the culture supernatants of AML12 cells (n = 4). IL-6, interleukin-6; IL-1β,interleukin-1β; TNF-α, tumor necrosis factor-α; $^{*}P < 0.05$; $^{**}P < 0.01$; $^{***}P < 0.001$; $^{\#\#\#}P < 0.001$; OV, overexpression; NC, negative control; ns, no significance

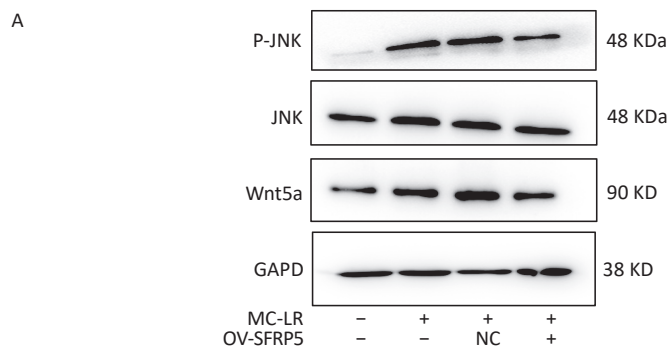

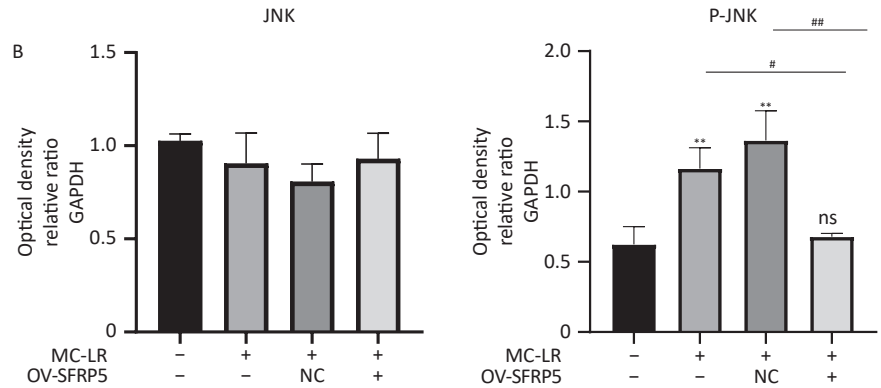

Figure 13. Overexpression of SFRP5 represses Wnt5a expression and JNK phosphorylation Representative blots and quantitative analysis of Wnt5a (A), JNK (B), and P- JNK (C). GAPDH, glyceraldehyde-3-phosphate dehydrogenase; JNK, Jun N-terminal kinase; P-JNK, phosphorylation-Jun N-terminal kinase; $^{*}P < 0.05$; $^{\#\#}P < 0.01$; OV, overexpression; NC, negative control; ns, no significance.

Received: November 9, 2023;
Accepted: March 6, 2024

REFERENCES

1. Frangež R, Kosec M, Sedmak B, et al. Subchronic liver injuries caused by microcystins. Pflügers Arch, 2000; 440, R103−4.
2. Fawell JK, Mitchell RE, Everett DJ, et al. The toxicity of cyanobacterial toxins in the mouse: I microcystin-LR. Hum Exp Toxicol, 1999; 18, 162−7.
3. Chen G, Yu SZ, Wei GR, et al. Studies on microcystin contents in different drinking water in highly endemic area of liver cancer. Chin J Prev Med, 1996; 30, 6−9. (In Chinese)
4. He J, Li GY, Chen J, et al. Prolonged exposure to low-dose microcystin induces nonalcoholic steatohepatitis in mice: a systems toxicology study. Arch Toxicol, 2017; 91, 465−80.
5. Finucane MM, Stevens GA, Cowan MJ, et al. National, regional, and global trends in body-mass index since 1980: systematic analysis of health examination surveys and epidemiological studies with 960 country-years and 9·1 million participants. Lancet, 2011; 377, 557−67.
6. Wang Q, Niu Y, Xie P, et al. Factors affecting temporal and spatial variations of microcystins in Gonghu Bay of Lake Taihu, with potential risk of microcystin contamination to human health. Sci World J, 2010; 10, 348387.
7. Zhang XJ, Chen C, Ding JQ, et al. The 2007 water crisis in Wuxi, China: analysis of the origin. J Hazard Mater, 2010; 182, 130−5.
8. Grabner GF, Xie H, Schweiger M, et al. Lipolysis: cellular mechanisms for lipid mobilization from fat stores. Nat Metab, 2021; 3, 1445−65.
9. Du C, Zheng SL, Yang Y, et al. Chronic exposure to low concentration of MC-LR caused hepatic lipid metabolism disorder. Ecotoxicol Environ Saf, 2022; 239, 113649.
10. Geng YN, Faber KN, de Meijer VE, et al. How does hepatic lipid accumulation lead to lipotoxicity in non-alcoholic fatty liver disease?. Hepatol Int, 2021; 15, 21−35.
11. Piché ME, Tchernof A, Després JP. Obesity phenotypes, diabetes, and cardiovascular diseases. Circ Res, 2020; 126, 1477−500.
12. Hu YF, Chen J, Fan HH, et al. A review of neurotoxicity of microcystins. Environ Sci Pollut Res Int, 2016; 23, 7211−9.
13. Wang XJ, Zhang X, Chu ESH, et al. Defective lysosomal clearance of autophagosomes and its clinical implications in nonalcoholic steatohepatitis. FASEB J, 2018; 32, 37−51.
14. Li Y, Rankin SA, Sinner D, et al. Sfrp5 coordinates foregut specification and morphogenesis by antagonizing both canonical and noncanonical Wnt11 signaling. Genes Dev, 2008; 22, 3050−63.
15. Chatani N, Kamada Y, Kizu T, et al. Secreted frizzled-related protein 5 (Sfrp5) decreases hepatic stellate cell activation and liver fibrosis. Liver Int, 2015; 35, 2017−26.
16. Mori H, Prestwich TC, Reid MA, et al. Secreted frizzled-related protein 5 suppresses adipocyte mitochondrial metabolism through WNT inhibition. J Clin Invest, 2012; 122, 2405−16.
17. Akoumianakis I, Sanna F, Margaritis M, et al. Adipose tissue-derived WNT5A regulates vascular redox signaling in obesity via USP17/RAC1-mediated activation of NADPH oxidases. Sci Transl Med, 2019; 11, eaav5055.
18. Hirosumi J, Tuncman G, Chang L, et al. Author correction: a central role for JNK in obesity and insulin resistance. Nature, 2023; 619, E25.
19. Pal M, Febbraio MA, Lancaster GI. The roles of c-Jun NH_2-terminal kinases (JNKs) in obesity and insulin resistance. J Physiol, 2016; 594, 267−79.
20. Wang CP, Yu TH, Wu CC, et al. Circulating secreted frizzled-related protein 5 and chronic kidney disease in patients with acute ST-segment elevation myocardial infarction. Cytokine, 2018; 110, 367−73.
21. Chen LL, Zhao XL, Liang GJ, et al. Recombinant SFRP5 protein significantly alleviated intrahepatic inflammation of nonalcoholic steatohepatitis. Nutr Metab (Lond), 2017; 14, 56.
22. Sedan D, Laguens M, Copparoni G, et al. Hepatic and intestine alterations in mice after prolonged exposure to low oral doses of Microcystin-LR. Toxicon, 2015; 104, 26−33.
23. Yi XP, Xu SS, Huang FY, et al. Effects of chronic exposure to microcystin-LR on kidney in mice. Int J Environ Res Public Health, 2019; 16, 5030.
24. Xu SS, Yi XP, Liu WY, et al. A review of nephrotoxicity of microcystins. Toxins (Basel), 2020; 12, 693.
25. Jensen-Urstad APL, Semenkovich CF. Fatty acid synthase and liver triglyceride metabolism: housekeeper or messenger?. Biochim Biophys Acta Mol Cell Biol Lipids, 2012; 1821, 747−53.
26. Wang M, Ma LJ, Yang Y, et al. n-3 Polyunsaturated fatty acids for the management of alcoholic liver disease: A critical review. Crit Rev Food Sci Nutr, 2019; 59, S116−29.
27. ALJohani AM, Syed DN, Ntambi JM. Insights into stearoyl-CoA

desaturase-1 regulation of systemic metabolism. Trends Endocrinol Metab, 2017; 28, 831–42.
28. Sampath H, Ntambi JM. Role of stearoyl-CoA desaturase-1 in skin integrity and whole body energy balance. J Biol Chem, 2014; 289, 2482–8.
29. Sheng DD, Zhao SM, Gao L, et al. BabaoDan attenuates high-fat diet-induced non-alcoholic fatty liver disease via activation of AMPK signaling. Cell Biosci, 2019; 9, 77.
30. Chen LY, Duan YQ, Wei HQ, et al. Acetyl-CoA carboxylase (ACC) as a therapeutic target for metabolic syndrome and recent developments in ACC1/2 inhibitors. Expert Opin Investig Drugs, 2019; 28, 917–30.
31. Menendez JA, Lupu R. Fatty acid synthase and the lipogenic phenotype in cancer pathogenesis. Nat Rev Cancer, 2007; 7, 763–77.
32. Du QQ, Liu P, Zhang CY, et al. FASN promotes lymph node metastasis in cervical cancer via cholesterol reprogramming and lymphangiogenesis. Cell Death Dis, 2022; 13, 488.
33. Gonzalez-Bohorquez D, López IMG, Jaeger BN, et al. FASN-dependent de novo lipogenesis is required for brain development. Proc Natl Acad Sci USA, 2022; 119, e2112040119.
34. Gomez-Diaz C, Bargeton B, Abuin L, et al. A CD36 ectodomain mediates insect pheromone detection via a putative tunnelling mechanism. Nat Commun, 2016; 7, 11866.
35. Chen YL, Zhang J, Cui WG, et al. CD36, a signaling receptor and fatty acid transporter that regulates immune cell metabolism and fate. J Exp Med, 2022; 219, e20211314.
36. Zhan T, Rindtorff N, Boutros M. Wnt signaling in cancer. Oncogene, 2017; 36, 1461–73.
37. Lin JT, Song T, Li C, et al. GSK-3β in DNA repair, apoptosis, and resistance of chemotherapy, radiotherapy of cancer. Biochim Biophys Acta Mol Cell Res, 2020; 1867, 118659.
38. Ren J, Feng XM, Guo YN, et al. GSK-3β/β-catenin pathway plays crucial roles in the regulation of NK cell cytotoxicity against myeloma cells. FASEB J, 2023; 37, e22821.
39. Sen M, Lauterbach K, El-Gabalawy H, et al. Expression and function of wingless and frizzled homologs in rheumatoid arthritis. Proc Natl Acad Sci USA, 2000; 97, 2791–6.
40. Solinas G, Becattini B. JNK at the crossroad of obesity, insulin resistance, and cell stress response. Mol Metab, 2017; 6, 174–84.